

Electrical transport in doped polypyrrole films at low temperature

A. K. Meikap, A. Das, and S. Chatterjee

Indian Association for the Cultivation of Science, Materials Science Department, Jadavpur, Calcutta 700 032, India

M. Digar and S. N. Bhattacharyya

Indian Association for the Cultivation of Science, Polymer Science Unit, Jadavpur, Calcutta 700 032, India

(Received 1 July 1992)

We report the results of a comprehensive study of localization and electron-electron interaction effects in doped polypyrrole films. We have measured the electrical conductivity and magnetoconductivity within the temperature range $1.8 \text{ K} \leq T \leq 300 \text{ K}$. The observed temperature dependence of dc conductivity cannot be explained either by the band-conduction model or by assuming a temperature-dependent energy gap. However, the conductivity when temperature $T > 10 \text{ K}$ can be explained by Mott's variable-range hopping model and the density of states and hopping distance can be calculated from these data. The low-temperature conductivity obeys a $T^{1/2}$ law, which is explained by three-dimensional localization and an electron-electron interaction. Magnetoconductivity data indicate that the electron-electron-interaction effect is most prominent in doped polypyrrole films at low temperature. From the magnetoconductivity we have calculated the inelastic and spin-orbit-scattering time. The spin-orbit scattering is found to be independent of temperature and small in comparison with the inelastic scattering. Like three-dimensional amorphous metals the inelastic scattering field obeys a T^p ($p \approx 2$) law at low temperature.

I. INTRODUCTION

In recent years conducting polymer films have attracted considerable attention both to physicists and chemists because of the fact that these materials find wide applications in solid-state devices such as solar cells, Schottky junctions, electromagnetic interference shielding, batteries, sensors, and microelectronics.¹ In particular, this has been stimulated by the experimental finding that the electrical conductivity of certain polymers can be varied by about 16 orders of magnitude upon doping.² Therefore the process of conduction depends upon the synthesis, the dopant, the doping level, and the temperature range. In order to understand the transport mechanisms in conducting polymers many authors³⁻⁶ have given a number of theoretical models. Bloor³ suggested that the electrical properties of conducting polymers are influenced by conjugation, i.e., the chemical unsaturation of the carbon atoms of the polymer chain. Sun and co-workers⁷ explained the transport mechanism in conducting polymers such as *trans*-polyacetylene (*trans*-PA) in light of soliton theory, in which the charged solitons having no spin are responsible for electrical conduction. Independent theoretical models have been put forward by Su and co-workers⁴ and Kivelson⁵ to describe the observed spinless conduction in *trans*-PA, but none of the existing models can give a satisfactory picture for the conduction process. Polypyrrole is a conducting polymer, which has a nondegenerate ground state. Although it is assumed that the polarons and the bipolarons are the dominant charge carriers in these polymeric conductors, the mechanism of conduction in polypyrrole (PPY) has not been yet conclusively established because of the persistent structural disorder of the polymer. Over the last few years, the electrical conduction mechanism in thin

films, high and low mobility of inorganic semiconductors, and compound semiconductors⁸ can be explained by this polaron theory. Based on this theory, Singh *et al.*⁹ also described an approach to explain the temperature dependence of ac conductivity of lightly doped PPY films over a wide range of frequency and temperature. In a previous¹⁰ work the dc conductivity and thermoelectric power of electrochemically prepared PPY films having different thicknesses have been studied within the temperature range $90 \text{ K} < T < 300 \text{ K}$ and it has been found that the variation of dc conductivity with temperature is best represented by Epstein's variable range hopping model (VRH). Singh and co-workers¹¹ also reported the dc electrical conductivity of lightly doped PPY films in the temperature range $77 \text{ K} < T < 300 \text{ K}$ and the same has been explained in terms of Mott's variable range hopping theory. It is well known that at ultralow temperature the logarithmic variation of resistivity in two-dimensional disordered systems is explained by the theory of weak electron localization and electron-electron interaction. The first quantum effect is destroyed by the application of a magnetic field and leads to a negative magnetoresistance; however, the second interaction effect is not affected by the external low magnetic field and produces positive magnetoconductance. The possibility of two-dimensional localization in inhomogeneously iodine-doped polyacetylene is explained by Epstein *et al.*¹² However, Thummes and co-workers¹³ have shown $T^{1/2}$ variation of conductivity at low temperatures of potassium-doped polyacetylene. They interpreted these results in light of three-dimensional localization and electron-electron interaction theory.^{14,15}

In the present paper we report a detailed experimental study containing temperature-dependent conductivity and magnetoconductance of doped polypyrrole films in

the temperature range $1.8 \text{ K} \leq T \leq 300 \text{ K}$. From electrical conductivity measurements we calculate the hopping distance, screening factor, and density of states. Different scattering rates are also calculated from the magnetoconductance measurements.

II. THEORY

The doped polymers are termed synthetic metals in view of the high conductivity of these materials, but the temperature coefficient of resistivity is opposite to that of metals. The conductivity is generally explained by a variable range hopping model⁸ originally proposed for semiconductors. On the assumption of phonon-assisted hopping between localized states in the VRH model the electrical conductivity can be written as

$$\sigma(T) = \sigma_0 \exp[-(T_0/T)^\gamma]. \quad (1)$$

The exponent γ in the above equation is connected with the dimensionality of the charge transport in the solid. γ is $\frac{1}{4}$ for three-dimensional and $\frac{1}{3}$ for two-dimensional transport. For three-dimensional transport

$$T_0 = 24 / [\pi r_0^3 k_B N(E_f)], \quad (2)$$

$$\sigma_0 = \frac{3}{4} e^2 \gamma_0 R^2 N(E_f), \quad (3)$$

where r_0 is the localization length, k_B the Boltzmann constant, $N(E_f)$ the density of states at the Fermi surface, and $\gamma_0 (= 10^{12} - 10^{13} \text{ s}^{-1})$ the molecular vibration frequency. The hopping distance R is defined by Mott and Davis⁸ as

$$R = [3r_0 / 2\pi N(E_f) k_B T]^{1/4}. \quad (4)$$

At low temperature the conductivity of the three-dimensional amorphous system has been extensively investigated.¹⁶⁻¹⁸ It has been shown that due to interaction effects or localization the temperature-dependent part of the conductivity can be written as

$$\sigma(T) = A_0 + CT^{1/2}, \quad (5)$$

where A_0 and C are constant. For prominent interaction effects C is given by

$$C = 1.3e^2 / 4\pi^2 \hbar [\frac{4}{3} - \frac{3}{2}F] (k_B / 2\hbar D)^{1/2}. \quad (6)$$

The factors $\frac{4}{3}$ and $-\frac{3}{2}F$ result from exchange and Hartree contributions, with $0 < F < 1$; D is the diffusion factor which is given by the relation

$$D = \sigma / [e^2 N(E_f)]. \quad (7)$$

The three-dimensional magnetoconductance due to localization and electron-electron interaction can be written as

$$\begin{aligned} \Delta\sigma(H, t) = & -C_I T^{1/2} g_3(g\mu_B H / k_B T) \\ & -C_L H^{1/2} \{ 0.5f_3(H/H_i) \\ & - 1.5f_3[H/(H_i + 2H_{so})] \}, \quad (8) \end{aligned}$$

where

$$\begin{aligned} C_I &= e^2 / 2\pi^2 \hbar (k_B / 2\hbar D)^{1/2} \tilde{F}_\sigma, \\ C_L &= (e^2 / 2\pi^2 \hbar) (e / \hbar C)^{1/2}, \\ \tilde{F}_\sigma &= 8(1 + F/2) \ln(1 + F/2) / F - 4. \end{aligned} \quad (9)$$

The functions $f_3(x)$ and $g_3(x)$ are defined in Refs. 14 and 15, respectively. Here the magnetoconductance for a particular temperature can be defined as $\Delta\sigma(H, T) = \sigma(H, T) - \sigma(0, T)$ and the different scattering rates are related with the scattering field by the relation

$$\tau_x = \hbar / (4eDH_x), \quad (10)$$

where $x = i$, so corresponding to inelastic scattering and spin-orbit scattering, respectively.

III. SAMPLE PREPARATION AND EXPERIMENTAL TECHNIQUE

Pyrrrole (Eastman Organic Chemicals, USA) was distilled at a reduced pressure of 60–70 mm of Hg. The middle portion of the distillate was collected, transferred in a number of small tubes, degassed in a vacuum line ($< 10^{-5}$ Torr), sealed, and stored in darkness at -10°C . Acetonitrile (E. Merck, Germany) and tetrabutyl ammonium tetra fluoroborate (Bu_4NBF_4) (Fluka) were used as received.

Polypyrrole films were prepared by electrochemical oxidation of pyrrole on Pt anodes ($2.5 \text{ cm} \times 1.4 \text{ cm}$) (cathodes were also Pt) with a constant potential of 2.3 V impressed between the Pt electrodes placed 1 cm apart in a one-compartment cell which contained a solution of pyrrole (0.1 M) and Bu_4NBF_4 (0.1 M) in acetonitrile. In order to make smooth films, one drop of concentrated sulfuric acid was added to the electrolyte solution. Before polymerization, the solution was deoxygenated by purging with nitrogen gas for 15 min and electrooxydative polymerization was carried out with a very slow bubbling of nitrogen gas just below the solution surface from behind the counter electrode. Films of different thickness were prepared by varying the polymerization time. After polymerization, films were washed with acetone, peeled off from the electrode surface with a razor blade, washed again several times with acetone, and dried in a vacuum at room temperature for 72 h. For physical measurements, films obtained on the surface of the anode facing the counter electrode were always used.

The films of different thickness are used to measure the electrical conductivity and magnetoresistance in the temperature range $1.8 \text{ K} \leq T \leq 300 \text{ K}$. The low-temperature measurement is performed using a He^4 cryostat equipped with an 8 T superconducting magnet. Our experiment was performed with a perpendicular magnetic field. The temperature is reduced below 4.2 K by pumping and it is stabilized by a pressure regulator. For other temperatures $T > 4.2 \text{ K}$ the sample is heated through a temperature controller. The magnetic field is measured by measuring the current through the superconducting coil. The resistance is measured by applying the standard four-terminal voltage technique, using a Keithley 220 programmable current source coupled to a nanovoltmeter. Fine copper wire and silver paint are used for electri-

cal connections. The current level is low enough to avoid self-heating. This four-terminal technique is used for avoiding complications arising from contact resistances. The resistivity ρ of the sample is determined from the formula $\rho = Rbd/l$, where b , d , and l are the width, thickness, and length of the sample, respectively.

IV. RESULTS AND DISCUSSION

We have measured electrical resistance and magnetoresistance of polypyrrole films in the temperature range $1.8 \text{ K} \leq T \leq 300 \text{ K}$. The electrical conductivity of doped polypyrrole decreases with decreasing temperature, i.e., semiconductorlike behavior. The conductivity ratio $r (= \sigma_{300}/\sigma_{4.2})$ of the samples is very high, i.e., 3.01×10^4 for PPY1 and 3.32×10^3 for PPY2. This is shown in Fig. 1. Such conductivity behavior may be attributed by two types of conduction mechanisms, such as intrachain conductivity, which can be described by the conduction mechanism for the band model and by the hopping contribution between the chains, which has been visualized by Mott.¹⁹ An electron just below the Fermi level jumps normally to a state just above it with energy E and is transferred from one chain to an adjacent chain of which the wave function overlaps that of the first chain. Thus, the electrical transport along the molecular chain is easier than between the chain in PPY films. Therefore, the intrachain conductivity is larger than the hopping conductivity between the chains. Figure 2 shows the variation of activation energy as a function of temperature as calculated from Fig. 1. The temperature-dependent activation energy shows that the band conduction model is not sufficient to explain the conductivity of polypyrrole films. Therefore, one should consider a temperature-dependent energy gap, which may take a major role in the conduction mechanism. But if we consider the semiconductor theory for conductivity in which the energy gap changes with temperature, it is clearly

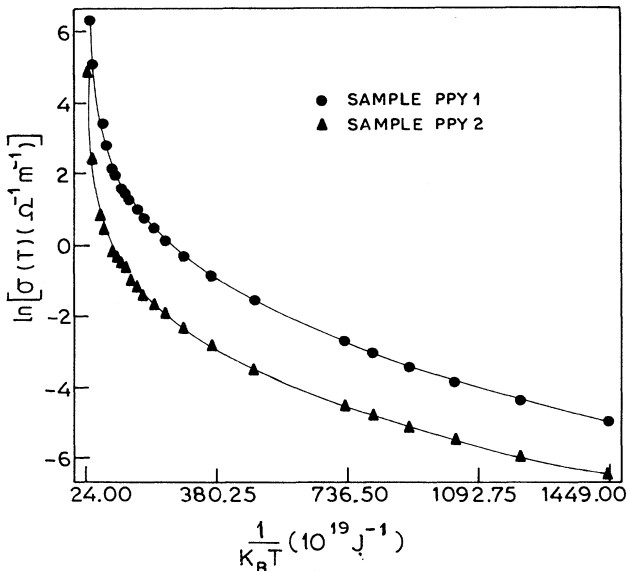


FIG. 1. Plot of $\ln \sigma_{dc}$ as a function of reciprocal temperature.

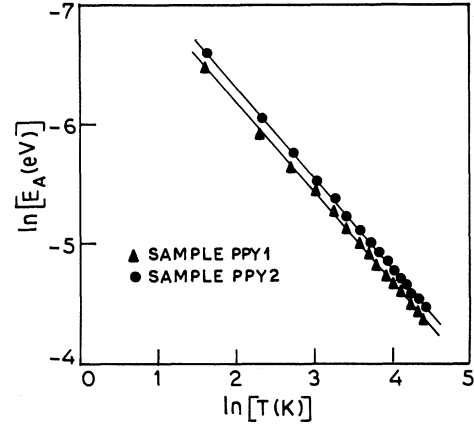


FIG. 2. Variation of calculated activation energy E_A as a function of temperature. These are plotted on a ln-ln scale.

seen that the temperature dependence of the energy gap has to be more than linear in order to account for the temperature dependence of activation energy. Hence the experimental results of polypyrrole films cannot be explained by considering a temperature-dependent band gap. On the other hand, if we consider the variable range hopping theory for conductivity as given in Eq. (1), the activation energy can be written as $E_A = \gamma k_B T \ln T^{-(\gamma-1)}$. A plot of $\ln E_A$ vs $\ln T$ represents a straight line with a slope $-(\gamma-1)$. Activation energy $E_A [= d \ln \sigma / d(1/k_B T)]$ has been calculated from the experimental data as shown in Fig. 1. We have also plotted the activation energy with temperature, which is shown in Fig. 2. From the figure we see that the plot of $\ln E_A$ vs $\ln T$ also represents a straight line. Finding the slope of these straight lines and comparing with $-(\gamma-1)$ we have estimated the values of γ to be $\frac{1}{4}$. Therefore, we may conclude that the hopping conduction may dominate the conduction mechanism in polypyrrole films and consequently we have analyzed our data by means of the VRH theory. We have fitted the experimental conductivity data with Eq. (1) taking σ_0 and T_0 as the fitting parameters with $\gamma = \frac{1}{4}$ and $\frac{1}{3}$, respectively. Values of σ_0 and T_0 are given in Table I. The solid lines in Figs. 3 and 4 represent the best-fitted theoretical values from Eq. (1) and the different points are the experimental data. It is clear from the figures that a good agreement has been observed between experimental and theoretical values of $\ln \sigma$ vs $T^{-1/4}$ establishing that the dc conduction mecha-

TABLE I. Physical parameters of doped polypyrrole films.

Sample parameters	PPY1	PPY2
Thickness (μm)	14.2	30.9
T_0 (K)	202 263	126 872
$N(E_f)$ (states/eV/cm ³)	4.38×10^{20}	6.98×10^{20}
D (cm ² /s)	0.065 4	0.013 2
H_i (T) at 4.2 K	0.516 94	0.620 04
H_{s0} (T)	0.077 4	0.075 3
\bar{F}_σ	0.78	0.78
γ_0 (s ⁻¹)	2.93×10^{13}	1.10×10^{12}
σ_0 ($\Omega^{-1} \text{m}^{-1}$)	10 023	4 459

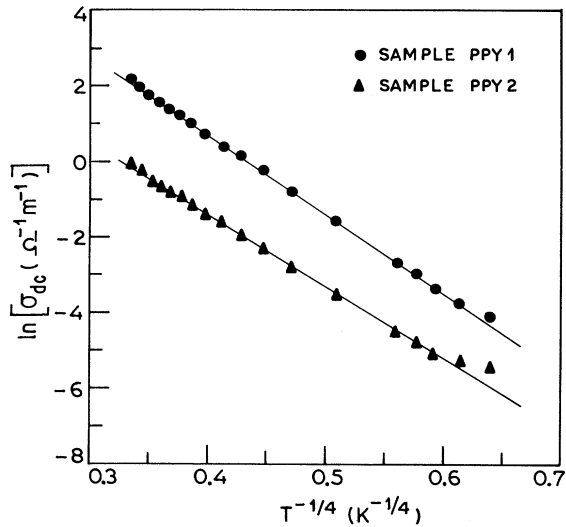


FIG. 3. Plot of $\ln\sigma_{dc}$ as a function of $T^{-1/4}$ for different samples. The solid lines are the best-fitted lines with Eq. (1) for $\gamma = \frac{1}{4}$.

nism in polypyrrole films is essentially determined by a three-dimensional hopping model. Electron diffraction studies²⁰ as well as x-ray photoelectron spectroscopy (XPS)²¹ and ultraviolet photoelectron spectroscopy (UPS)²² data show that polypyrrole is slightly disordered, producing an apparent localization of states in the band gap. Bredas *et al.*²³ have calculated that in polypyrrole the formation of a bipolaron which produces the conductivity in polypyrrole film is favored over two polarons by 0.45 eV and the bipolaron length is about four polypyrrole rings, which has been further verified by UPS²⁴ data. Therefore we assume that the hopping state is depolarized over four rings and the localization length r_0 is of the order of 10 Å. Now we have estimated the values of $N(E_f)$ and D from Eqs. (2) and (7), respectively, and given them in Table I. The estimated value of $N(E_f)$ is similar to that obtained from the ultraviolet spectroscopy.

py.²² The average hopping energy $E [= 3/4\pi R^3 N(E_f)]$ can be estimated by knowing the hopping distance R from Eq. (4) and density of states $N(E_f)$ from Table I. The calculation yields the value of R and E as 25.5 Å and 0.033 eV, respectively, for sample PPY1 and 22.7 Å and 0.029 eV, respectively, for sample PPY2. From the value of σ_0 we have estimated the molecular vibration frequency γ_0 from Eq. (3) and the values are shown in Table I.

The conductivity of the samples at low temperatures ($T < 5$ K) does not obey the above prediction. At low temperature the two quantum effects such as electron-electron interaction and weak electron localization are important for conductivity. It has been shown that due to localization or electron-electron interaction the temperature-dependent part of the conductivity is proportional to $\ln T$ for two-dimensional and $T^{1/2}$ for three-dimensional disordered systems. In order to evaluate the origin of this low-temperature anomaly of $\sigma(T)$ we have tried to fit $\sigma(T)$ curves in the temperature range 1.8 K $\leq T \leq 5$ K with the expressions $\sigma(T) \propto \ln T$ and $T^{1/2}$, respectively. This fit is shown in Figs. 5 and 6 where the solid lines correspond to $T^{1/2}$ and dashed lines correspond to $\ln T$. From the fitting it is clear that the conductivity obeys the $T^{1/2}$ law over the temperature range 1.8 K $\leq T \leq 5$ K. The fit yields the value of parameters $A_0 = 4.125 \times 10^{-3} \Omega^{-1} \text{m}^{-1}$ and $C = 5.55 \times 10^{-3} \Omega^{-1} \text{m}^{-1} \text{K}^{-1/2}$ for sample PPY1 and $A_0 = 1.28 \times 10^{-3} \Omega^{-1} \text{m}^{-1}$ and $C = 1.54 \times 10^{-3} \Omega^{-1} \text{m}^{-1} \text{K}^{-1/2}$ for sample PPY2, respectively. The positive value of C indicates that the exchange term exceeds the Hartree term of our systems. Inserting the values of C and D in Eq. (6) we can evaluate the screening parameter F which lies in the range $0 < F < 1$. Therefore we would like to point out that the three-dimensional interaction effect is dominant in the observed $T^{1/2}$ variation of conductivity.

The perpendicular magnetoresistance at different temperatures of the samples PPY1 and PPY2 is shown in Figs. 7 and 8, respectively. The magnetoconductance is negative at low temperatures and its magnitude decreases with an increase of temperature. Similar behavior is

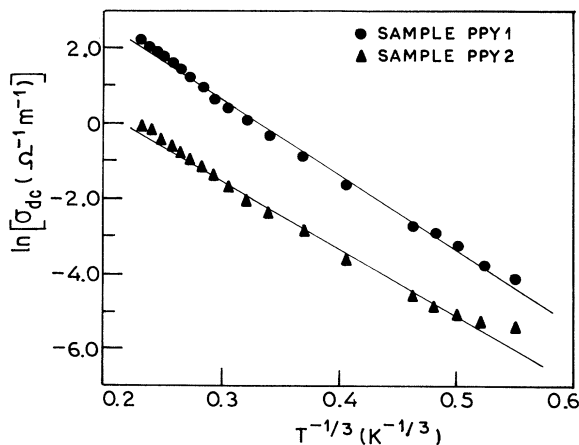


FIG. 4. Plot of $\ln\sigma_{dc}$ as a function of $T^{-1/3}$ for different samples. The solid lines are the best-fitted lines with Eq. (1) for $\gamma = \frac{1}{3}$.

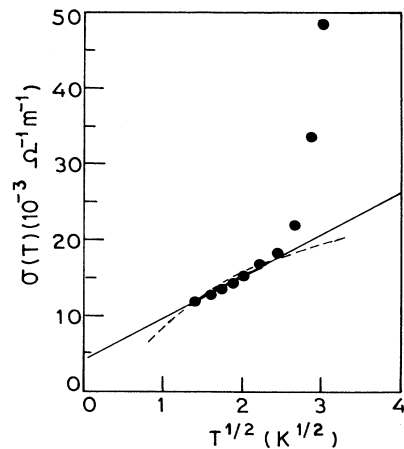


FIG. 5. Conductivity as a function of $T^{1/2}$ of PPY1. The solid and dashed lines are the best-fitted conductivity corresponding to $T^{1/2}$ and $\ln(T)$, respectively.

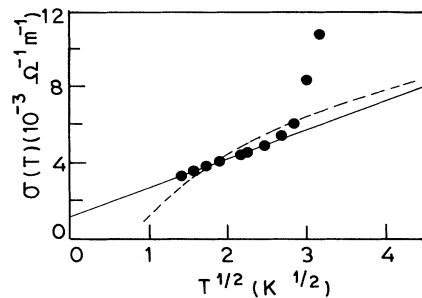


FIG. 6. Conductivity as a function of $T^{1/2}$ of PPY2. The solid and dashed lines are the best-fitted conductivity corresponding to $T^{1/2}$ and $\ln(T)$, respectively.

found in metallic films.²⁵ This results from the temperature dependence of inelastic scattering time $\tau_i \propto T^{-p}$. It is seen from Eq. (8) that magnetoconductance due to electron-electron interaction becomes important at high fields and low temperature. Here we discuss the observed magnetoconductance in terms of additive contributions from electron-electron interaction with spin ($g=2$) splitting and three-dimensional localization as given in Eq. (8). In order to calculate the different scattering fields such as inelastic scattering field (H_i) and spin-orbit scattering field (H_{so}), we have fitted the experimental magnetoconductance data with Eq. (8) using H_i and H_{so} as fitting parameters for a particular temperature. A typical least-squares fit is shown in Figs. 7 and 8. The solid lines are the theoretical curves obtained from Eq. (8) and different points are the experimental data. Figures 7 and 8 show a good agreement between theory and experiment regarding magnetoconductance in the temperature range $1.8 \text{ K} \leq T \leq 5 \text{ K}$, where the $\sigma(T)$ vs $T^{1/2}$ law holds. The values of different scattering times, i.e., inelastic (τ_i) and spin-orbit (τ_{so}), are calculated from Eq. (10) using the

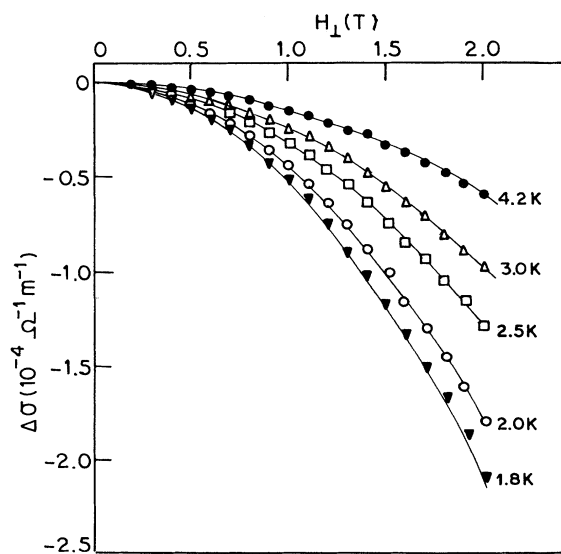


FIG. 7. Magnetoconductivity as a function of perpendicular magnetic field of PPY1 for constant different temperature. The solid line represents fits to Eq. (8).

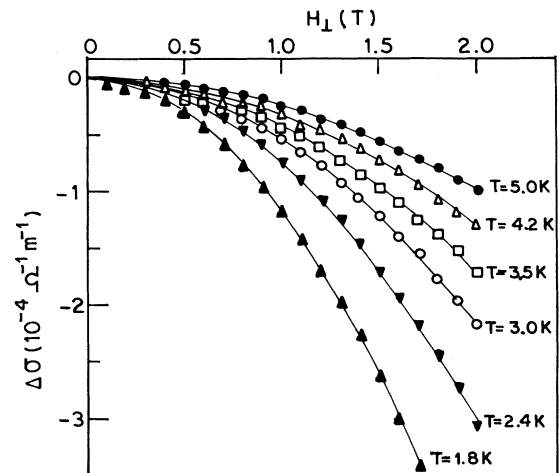


FIG. 8. Magnetoconductivity as a function of perpendicular magnetic field of PPY2 for constant different temperature. The solid line represents fits to Eq. (8).

best-fitted values of the parameters H_i and H_{so} . The values of these scattering fields are shown in Table I. The fitting of magnetoconductance yields $H_{so} < H_i$; i.e., the spin-orbit scattering is weaker than the inelastic scattering. According to the predication of Abrokosov and Gorkov,²⁶ the spin-orbit scattering depends on the atomic no. (Z). In polypyrrole films the atomic numbers of the constituent elements are comparatively small. Due to this the spin-orbit scattering is small in polypyrrole films. In the case of weak spin-orbit scattering the contribution to magnetoconductance from localization produces the positive magnetoconductance. However, in our polypyrrole films we observe a negative magnetoconductance. This result suggests that the magnetoconductance due to electron-electron interaction is more prominent than the localization contribution.

The temperature dependence of the inelastic scattering time of polypyrrole film of different thicknesses is shown in Fig. 9. The inelastic scattering arises due to two im-

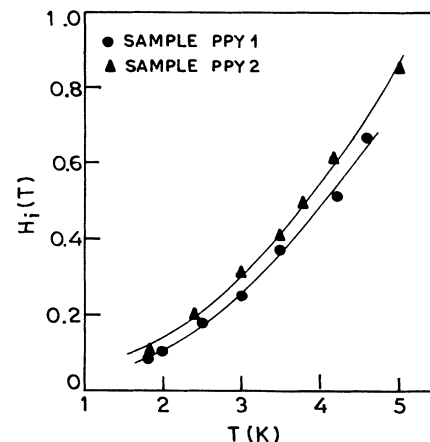


FIG. 9. The temperature dependence of the inelastic scattering field (H_i) of PPY1 and PPY2 films. The solid line shows the relation of $H_i \propto T^p$ with $p \approx 2$.

portant mechanisms: one is electron-phonon scattering (τ_{e-p}^{-1}) and the other is electron-electron scattering (τ_{e-e}^{-1}). There is a general theoretical prediction that in three-dimensional systems the electron-phonon scattering time (τ_{e-p}^{-1}) should go as T^3 . However, the standard result of the electron-electron scattering rate in three-dimensional systems is proportional²⁷ to T^2 . In order to understand the inelastic scattering mechanism at low temperatures ($1.8 \text{ K} \leq T \leq 5 \text{ K}$), we have tried to fit the inelastic scattering field (H_i) of the polypyrrole film with the equation $H_i = AT^p$ with A and p as fitting parameters. The fit yields the value of $p \approx 2$. This result is found similarly for amorphous metallic films.²⁸ Therefore we could conclude that the inelastic scattering mechanism in polypyrrole films in the temperature range $1.8 \text{ K} \leq T \leq 5 \text{ K}$ is due to the electron-electron scattering mechanism ($p = 2$) and not due to electron-phonon scattering ($p = 3$).

V. CONCLUSION

In this work we have studied the transport properties of conducting polypyrrole films. The dc electrical conductivity is measured in the temperature range $1.8 \text{ K} \leq T \leq 300 \text{ K}$. The observed temperature dependence of dc conductivity cannot be explained either by the band conduction model or by assuming a temperature-dependent energy gap. However, the conductivity in the

temperature range $T > 10 \text{ K}$ can be explained by Mott's variable range hopping model for disordered systems in which the polaronic hopping conduction is the dominant conduction mechanism. This yields the value of density of states $N(E_f)$ and diffusion constant D that agree well with the values of other conjugate polymers. At low temperatures the dc conductivity of the polypyrrole film obeys a $T^{1/2}$ law. The magnetic field and temperature dependence of conductivity are dominated by two quantum effects arising from electron localization and electron-electron interaction at low temperatures. From magnetoconductance data we have calculated different scattering fields: i.e., the inelastic scattering field (H_i) and the spin-orbit scattering field (H_{so}). The spin-orbit scattering field does not depend on temperature and is smaller than the inelastic scattering field. The inelastic scattering field obeys the relation $H_i \propto T^p$ with $p \approx 2$. Therefore, at low temperatures, i.e., $1.8 \text{ K} \leq T \leq 5 \text{ K}$ the inelastic scattering time originates only from an electron-electron interaction.

ACKNOWLEDGMENTS

This work was performed under a grant by the Department of Science and Technology, Government of India. We wish to acknowledge our gratitude for this financial support during this work.

¹K. R. Schoch, Jr., *IEEE Electron. Ins. Magn.* **2**, 20 (1986).

²J. W. C. Chien, *Polyacetylene* (Academic, Orlando, 1984).

³D. Bloor, *IEE Proc.* **130**, 225 (1983).

⁴W. P. Su, J. R. Schrieffer, and A. J. Heeger, *Phys. Rev. B* **22**, 2099 (1981).

⁵S. Kivelson, *Phys. Rev. B* **25**, 3793 (1982).

⁶S. Kivelson, *Mol. Cryst. Liq. Cryst.* **77**, 65 (1983).

⁷S. Sun, L. Chen, and E. X. Yu, *Solid State Commun.* **53**, 973 (1985).

⁸N. F. Mott and E. A. Davis, *Electronic Processes in Non Crystalline Materials* (Clarendon, London, 1979).

⁹R. Singh, R. P. Tandon, V. S. Panwar, and S. Chandra, *J. Appl. Phys.* **69**, 2504 (1991).

¹⁰R. Roy, S. K. Sen, M. Digar, and S. N. Bhattacharyya, *J. Phys. Condens. Matter* **3**, 7849 (1991).

¹¹R. Singh, R. P. Tandon, and S. Chandra, *J. Appl. Phys.* **70**, 243 (1991).

¹²A. J. Epstein, H. W. Gilson, P. M. Chalkin, W. G. Clark, and G. Gruner, *Phys. Rev. Lett.* **45**, 1730 (1980).

¹³G. Thummes, F. Korner, and J. Kotzler, *Solid State Commun.* **67**, 215 (1982).

¹⁴A. Kawabata, *Solid State Commun.* **34**, 431 (1980).

¹⁵P. A. Lee and T. V. Ramakrishnan, *Rev. Mod. Phys.* **57**, 287 (1985).

¹⁶E. Abraham, P. W. Anderson, D. C. Licciardell, and T. V. Ramakrishnan, *Phys. Rev. Lett.* **42**, 673 (1979); Y. Imry, *J.*

Appl. Phys. **52**, 1817 (1981).

¹⁷B. L. Altshuler and A. J. Aronov, *Zh. Eksp. Teor. Fiz.* **77**, 2028 (1979) [*Sov. Phys. JETP* **50**, 968 (1979)].

¹⁸M. Kaveh, and N. F. Mott, *J. Phys. C* **14**, 2183 (1981); **14**, 4177 (1981).

¹⁹N. F. Mott, *Metal Insulator Transitions* (Taylor and Francis, London, 1974).

²⁰R. H. Geiss, G. W. Street, W. Volkenson, and J. Economy, *IBM J. Res. Dev.* **27**, 321 (1983).

²¹P. Pfluger, M. Krounbi, G. B. Street, and G. Weiser, *J. Chem. Phys.* **78**, 3212 (1983); P. Pfluger and G. B. Street, *ibid.* **80**, 544 (1984).

²²P. Pfluger, U. M. Gubler, and G. B. Street, *Solid State Commun.* **49**, 911 (1984).

²³J. L. Bredas, K. Yakushi, J. C. Scott, and G. B. Street, *Phys. Rev. B* **30**, 1023 (1984).

²⁴W. K. Ford, C. W. Duke, and W. R. Salocneck, *J. Chem. Phys.* **77**, 5030 (1982).

²⁵A. K. Meikap, A. R. Jana, S. K. De, and S. Chatterjee, *Solid State Commun.* **77**, 249 (1991).

²⁶A. Abrikosov and L. P. Gorkov, *Zh. Eksp. Teor. Fiz.* **42**, 1088 (1962) [*Sov. Phys. JETP* **15**, 752 (1962)].

²⁷N. W. A. Shroft and N. D. Mermin, *Solid State Physics* (Holt, Rinehart, and Winston, New York, 1976).

²⁸B. J. Hickey, D. Greig, and M. A. Howson, *Phys. Rev. B* **36**, 3074 (1987).